Atmospheric Environment 253 (2021) 118389

Contents lists available at ScienceDirect

Atmospheric Environment

journal homepage: http://www.elsevier.com/locate/atmosenv

The abundance and characteristics of atmospheric microplastic deposition in the northwestern South China Sea in the fall

Yongcheng Ding [a,b], Xinqing Zou [a,b,c,*], Chenglong Wang [a,b], Ziyue Feng [a,b], Ying Wang [a,b], Qinya Fan [a,b], Hongyu Chen [a,b]

[a] School of Geography and Ocean Science, Nanjing University, Nanjing, 210023, China
[b] Ministry of Education Key Laboratory for Coastal and Island Development, Nanjing University, Nanjing, 210023, China
[c] Collaborative Innovation Center of South China Sea Studies, Nanjing University, Nanjing, 210023, China

HIGHLIGHTS

- Dry deposition of atmospheric MPs into the northwestern SCS in the fall was 1400 t.
- The number of MPs gradually increased and peaked as the particle size decreased.
- The airflow may carry MPs over cities in southeastern China into SCS in the fall.
- Long-term monitoring of atmospheric MPs and making evaluation standards are needed.

ARTICLE INFO

Keywords:
Northwestern South China Sea
Atmospheric microplastics
Airflow
Deposition
Source

ABSTRACT

Atmospheric microplastics have been widely reported and detected in remote mountain areas and oceans, indicating that they can be transported over long distances through the atmosphere. Regional transport and deposition processes of atmospheric microplastics have a significant impact on the source and sink patterns, as well as the flux mechanisms of microplastics in terrestrial and marine environments. However, few studies have been conducted on the deposition of atmospheric microplastics. Thus, in this study, we collected atmospheric microplastic samples from the northwestern South China Sea and estimated that in the fall the dry deposition of atmospheric microplastics into the ocean was 1.4×10^3 t, which had a greater contribution than riverine inputs of microplastics in this region, suggesting that atmospheric microplastics are non-negligible sources of marine plastic litter with high environmental risk. Additionally, we reported on the abundance (0.035 ± 0.015 n/m^3), morphological characteristics, composition, and sources of atmospheric microplastics in the northwestern South China Sea. Smaller-sized microplastics had a high abundance that decreased with increased proximity from the coast. Most of the detected microplastics were fibers, which accounted for approximately two-thirds of the total quantity. The spectral analysis detected seven polymer types, and polyester was predominant (29%). Combined with the cluster analysis of the backward trajectories of airflow, we demonstrated that the airflow affecting the northwestern South China Sea originated mainly from the northeast, potentially carrying microplastics from cities located in southeastern Chinese provinces to the South China Sea.

1. Introduction

The continually increasing total global plastic production reached approximately 359 million tons in 2018, with a compound growth rate of 4.1% over the past decade (Plastic Europe, 2019). According to current trends, approximately 12 billion tons of plastic waste will have been generated by 2050 (Geyer et al., 2017), while the amount of plastic waste entering the oceans is estimated to reach 32 million tons (World Economic Forum, 2016). As most plastic polymer types are highly resistant to aging and have very slow biodegradation rates (Moore, 2008), plastics will persist in the marine environments for as long as hundreds of years (Cózar et al., 2014). In addition, microplastics formed by the fragmentation of large plastics are highly susceptible to the attachment of pathogenic microorganisms (Rochman et al., 2015;

* Corresponding author. School of Geography and Ocean Science, Nanjing University, Nanjing, 210023, China.
E-mail address: zouxq@nju.edu.cn (X. Zou).

https://doi.org/10.1016/j.atmosenv.2021.118389
Received 10 November 2020; Received in revised form 7 March 2021; Accepted 30 March 2021
Available online 3 April 2021

Zettler et al., 2013), which can then be transmitted via the food chain during transport to the ocean, posing a potential hazard to marine organisms, birds, and human health (Jiang et al., 2018; Kiessling et al., 2015; Zhao et al., 2014). Hence, the resulting ocean pollution by microplastics has attracted widespread attention.

Currently, the main plastic sources in the marine environment are considered to be coastal land and riverine inputs (Jambeck et al., 2015; Lebreton et al., 2017). In 2010, the plastic waste generated and discarded into oceans by 192 coastal countries was between 4.8 and 12.7 million tons (Jambeck et al., 2015). Moreover, there are 1.15 and 2.41 million tons of plastic waste entering the ocean through rivers every year (Lebreton et al., 2017), and, over time, these plastics will gradually degrade into microplastics. Compared to coastal land and rivers, atmosphere is another important pathway for the regional and global transport of plastics, covering the entire ocean surface (Camarero et al., 2017; Chen et al., 2020; Evangeliou et al., 2020; GESAMP, 2016; Huang et al., 2020) and, based on current research, almost all of the plastics carried by the atmosphere are microplastics. (Allen et al., 2019; Cai et al., 2017; Dris et al., 2015; Liu et al., 2019a; Wang et al., 2019; Wright et al., 2020). Thus, atmospheric transport is also a potential source of microplastics in the marine environment.

Few studies focus on the atmospheric deposition of microplastics. Dris et al. (2015) first discovered the deposition of microplastics in the atmosphere around Paris. They proposed that wind can transport plastics to remote areas, thereby entering the marine environment eventually. Zhou et al. (2017) reported on the types, deposition fluxes, and seasonal changes of atmospheric microplastics in Yantai. They suggested that microplastics in the atmospheric environment of coastal cities may enter the land-sea environment through deposition, highlighting it as an important source of microplastics in marine and coastal environments. Cai et al. (2017) analyzed the role that the physical action of wind and chemical weathering may play on the degradation of atmospheric microplastics, they found that adhering particles, grooves, pits, fractures, and flakes were the common patterns of degradation. Liu et al. (2019a) investigated the basic characteristics of atmospheric microplastics in the Western Pacific using active sampling methods, and estimated the quality of atmospheric microplastics for the first time. Wang et al. (2019) conducted a transoceanic survey of 21 sampling transects ranging from the South China Sea to the East Indian Ocean. Their results suggested that microplastics can be transported over long distances (more than 1000 km) through the atmosphere.

Of the few studies on atmospheric microplastics, most explore issues such as distribution, composition, and long-distance transport (Zhang et al., 2019, 2020), with even fewer studies on the deposition of atmospheric microplastics into the ocean (Cai et al., 2017; Dris et al., 2015; Zhou et al., 2017). Therefore, the aims of this research were to 1) study the distribution, morphological characteristics, and composition of atmospheric microplastics in the northwestern South China Sea; 2) explore the possible atmospheric microplastic sources; and 3) estimate the quantity of microplastic deposited into the northwestern South China Sea in the fall. Additionally, we evaluated the contribution of dry deposition of atmospheric microplastics to the ocean to better assess the source and sink components of the system, as well as the potential effects of microplastics on the environment.

2. Material and methods

2.1. Study area

The sampling area was the northwestern South China Sea (17°–24°N, 110°–116°E) (Fig. 1). This is an area with a typical monsoon climate and is both an important part of the world's largest ocean thermal reservoir and a sensitive area in terms of sea–air interactions (Pidwirny, 2011). Additionally, this area is highly influenced by weather-related climate change in the northern hemisphere (He, 2016).

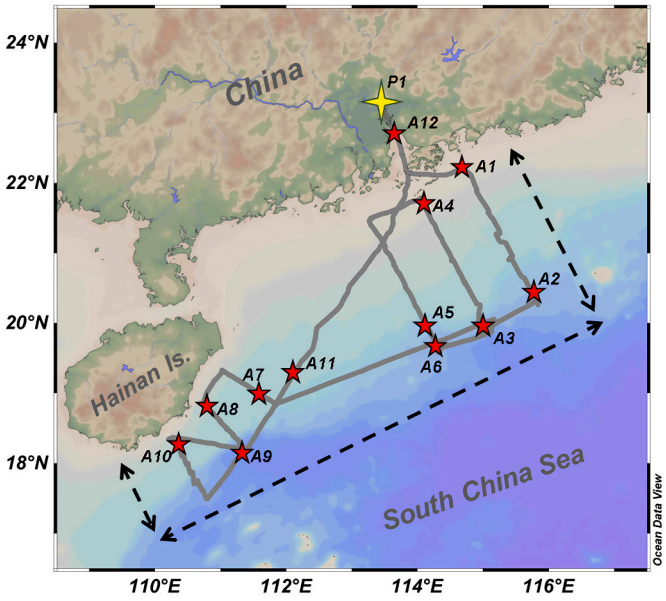

Fig. 1. Sampling area (the gray line represents the geo-location of the sampling track. The 12 five-pointed red stars represent the active sampling reception points and the four-pointed yellow star represents the passive sampling station. The area between the black dotted line and the coastline is the sampling area). (For interpretation of the references to color in this figure legend, the reader is referred to the Web version of this article.)

2.2. Air sampling

2.2.1. Active sampling

A total of 12 samples were collected during the South China Sea oceanographic research cruise (NORC2019-09) conducted by the scientific research vessel "SHIYAN 1" from September 26 to October 8, 2019. An active atmospheric sampler (Tisch TE-1000 PUF, Ohio, the United States) was used for atmospheric microplastic sampling throughout the cruise trajectory. This equipment was fixed at the highest part of the ship, approximately 10 m from the horizontal plane, and far from the chimney to avoid contamination (Fig. S1). The GF/A glass microfiber filter (Whatman, Kent, UK), with a pore size of 3 μm and diameter of 90 mm, was replaced every 12–25 h, and the sampling volume was calculated according to the formula provided by the sampler. The following was the general procedure. First, the sampler was calibrated to accurately quantify the filtered air volume according to the manufacturer's instructions (Liu et al., 2019b; Zhang et al., 2019). Next, the filter was placed tightly in an aluminum alloy sampling probe, which was screwed to the top of the sampler. The sampling probe was then covered with a large baffle to prevent the filters from being drenched in the rain. The surrounding air entered through the space under the baffle. Thereafter, the values for pressure gauges and schedules were recorded from the sampler system to calculate the gas volume (Text S1). When the sampling session ended, the filter was removed using stainless-steel tweezers and carefully placed in a glass culture dish (Normax, Marinha Grande, Portugal) (Wang et al., 2019). Finally, all filters were transferred to the laboratory for further analysis. Owing to weather conditions, all the valid samples were of atmospheric dry deposition origin.

2.2.2. Passive sampling

To better assess the atmospheric flux of microplastics into the ocean from the active sampling computational model, for comparison, we supplemented our data with passive sampling. The sampling collector was placed on top of the scientific research vessel "SHIYAN 1," which was docked in the Pearl River Estuary, where all active sampling was performed. The height from which samples were obtained was the same

as that used in the active sampling method. The sampling period ranged from October 24 to November 24, 2019. As shown in Fig. S1, six identical sampling collectors were placed in a tin box and secured to the side of the vessel. The rest of the procedures were the same as those followed during active sampling. The equations used to calculate the dry deposition of atmospheric microplastics in the passive sampling method are shown in Text S2.

2.3. Microplastic count and identification

We used stereomicroscopy (Leica Microsystems, Wetzlar, Germany) and Fourier transform infrared microspectroscopy (Nicolet iN10; Thermo Fisher Scientific, Waltham, MA, USA) to separate microplastics from other atmospheric aerosols.

First, the microplastics on the filters were initially inspected and counted with a stereomicroscope at 30–80× magnification according to their morphological characteristics (Text S3). To ensure the integrity of the statistical process, we mainly used the "zigzag" pattern to measure and count the microplastics and the particles suspected of being microplastics collected on the filters (Peng et al., 2017) (Fig. S2). Auxiliary visual methods were also used to ensure that the statistical results were as accurate as possible (Crawford and Quinn, 2017; Hidalgo-Ruz et al., 2012). The area of each flaky, irregularly shaped plastic particle had to be recorded by the stereomicroscope's read function. In this counting process, we also considered relevant parameters, such as shape and color of the microplastics.

Second, all the inspected and counted microplastics were selected and their composition identified using Fourier transform infrared microspectroscopy. The background interference was corrected prior to measurements, after which the detected spectrograms were compared against the OMNIC polymer reference spectral library (Käppler and Fischer, 2016; Mecozzi et al., 2016) (Fig. S3). The spectrograms were obtained in transmission mode. Samples with a matching rate >70% and suitable functional groups were accepted as microplastics. Solid aerosols that are not plastic components were directly excluded. As such, we could identify and separate all the microplastics collected on the GF/A glass microfiber filter.

2.4. Backward trajectory and cluster trajectory

To trace the areas through which the air masses passed before reaching the reception points as well as to analyze the dominant air flow directions and potential microplastic sources affecting the sampling area (Jiang et al., 2016; Zhu et al., 2016), we used the National Oceanic and Atmospheric Administration database and the Hybrid Single-Particle Lagrangian Integrated Trajectory (HYSPLIT) model, developed by the Australian Bureau of Meteorology, for air mass trajectory simulation and cluster analysis of all trajectories during sampling (Brankov et al., 1998). Backward trajectories have more integrated transport, dispersion, and deposition patterns that handle multiple meteorological input fields, physical processes, and different types of emission sources. Further, they have been used to study the transport and dispersion of microplastics in many areas (Allen et al., 2019; Liu et al., 2019b; Wang et al., 2019). As the accuracy of the single-root trajectory is always affected by the spatio-temporal resolution of the meteorological field and some assumptions used in the model, we combined it with cluster analysis to improve the accuracy of the results and characterize the pollution level in the area more precisely (Ma et al., 2015).

The backward airflow trajectories were calculated daily from September 26 to October 8, 2019 and each trajectory had a duration of 120 h (Fig. S4). The starting time of the backward trajectory calculation was in the middle of the daily sampling session (at approximately 00:00 GMT), and the 12 latitudes and longitudes corresponding to this time point were simulated as reception points (Fig. 1). The starting height of the backward trajectory was set to 10 m, which was roughly the same as the height used to collect atmospheric microplastics.

Subsequently, we simulated the backward trajectories of the 12 reception points using the multi-receptor mode. Additionally, we used data from the Global Data Assimilation System (GDAS) that covered the period from September 26 to October 8, 2019, which was part of the sampling period, to cluster 120-h backward trajectories. The trajectories were calculated 24 times a day at 1-h intervals and grouped according to their transport direction and velocity using the angular distance method. The distribution and transport characteristics of the trajectories were studied in conjunction with the analysis of the moving routes of the air masses. A detailed explanation of the cluster analysis process can be found in Text S4.

2.5. Dry deposition of atmospheric microplastics in the northwestern South China Sea

If driven by wind, microplastics can be carried over cities and even distant areas over the ocean. The contribution of dry-deposited atmospheric microplastics in the northwestern South China Sea was estimated by calculating the dry deposition velocity of microplastics in the atmosphere.

We used the data from active sampling and calculated the dry deposition velocity of atmospheric microplastics, as it hardly rained during the sampling period. Currently, the calculation of the dry deposition fluxes through the indirect estimation of dry deposition velocities is an important method for assessing the fluxes of atmospheric pollutants into the ocean (Wang, 2006; Zhan et al., 2010). The dry deposition model has become one of the most important means to obtain dry deposition velocity data (Sun et al., 2018). In this study, we calculated the deposition velocities of differently shaped atmospheric microplastics, based on the Williams model and various improved methods (Guo et al., 2005; Kukulka et al., 2012; Lo et al., 1999; SOA, 2015; Williams, 1982). Thereafter, we performed a quantitative evaluation of the dry deposition of microplastics in the northwestern South China Sea in the fall. The procedures used to estimate the amount of atmospheric microplastics into the sea using dry deposition models consisted of the following steps:

(1) Microplastics were reclassified into cylindrical, flaky, and near-spherical shapes, and the nominal diameter (Inter-Agency Committee, 1957) of each microplastic (Text S5) was calculated.
(2) Dry deposition velocities (νdi) of differently shaped microplastics in a certain particle size range (Text S6) were calculated.
(3) The particle size spectral distribution rate was obtained depending on the number of microplastics of different shapes and certain size ranges (Zhang and Zhou, 1995) (Table S2). The weighted dry deposition velocity of the microplastics was $\nu_d = \sum_{i=1}^{n} \nu di \times dri$ (ν_d, νdi, and dri represent the weighted dry deposition velocity, the dry deposition velocity and the particle size spectral distribution rate, respectively).
(4) The dry deposition fluxes for differently shaped microplastics were calculated using the following equation: $F = \nu_d \times C_i$ (F and C_i represent the dry deposition flux and the abundance of microplastics of different shapes, respectively) (Balkanski et al., 1993).
(5) The masses (M) of differently shaped microplastics (Text S7, Table S2) were calculated (Here, we considered 1.2 g/cm^3 as the density of microplastics) (Text S8).
(6) The dry deposition mass for differently shaped microplastics was calculated separately using the following equation: $W = F \times S_a \times M$ (W and S_a represent the dry deposition mass and the northwestern South China Sea area, respectively).
(7) The total dry deposition mass of atmospheric microplastics was calculated using the following formula: $W_t = W_c + W_f + W_s$ (W_t represents the total dry deposition mass of atmospheric

microplastics. W_c, W_f, and W_s represent the dry deposition mass of cylindrical, flaky, and near-spherical microplastics, respectively).

2.6. Quality control and quality assurance

Considering the actual sampling time for this study and the meteorological conditions throughout the year, we calculated the atmospheric microplastic deposition from September 1 to November 30 during the fall, as the meteorological conditions at this time were not significantly different from the actual sampling. To minimize contamination, we implemented strict operating rules. Prior to each sampling session, the glassware and filters were wrapped in aluminum foil and heated in a muffle furnace at 450 °C for 4 h (Liu et al., 2019b). In addition, the easily contaminated parts of the sampler were wrapped in aluminum foil (Lenz et al., 2015). The samples were collected immediately and stored in glass dishes while the collectors wore dust proof lab coats, disposable nitrile gloves, and masks. Glass dishes for sample storage were cleaned with test paper and 70% ethanol before use. When active sampling was performed on each sampling transect, a clean GF/A glass microfiber filter was placed next to the active atmospheric sampler, and these were covered with the baffle. Outdoor blank samples were obtained by this method. Blank experiments for indoor air contamination were also designed to evaluate and eliminate background pollution during microscopic examination and identification in a clean room. Additionally, dust proof lab coats were required in the clean room at all times. The additional six parallel sampling collectors were placed next to the passive sampling collectors and sampled simultaneously. By comparison with the standard spectrogram, solid aerosols that are not plastic components were directly excluded and samples with a matching rate >70% were considered to be microplastics.

2.7. Data analysis

The values of basic parameters, such as wind speed, wind direction, and temperature were provided by the real-time collector and the conductivity, temperature, and depth system (CTD) on-board the scientific research vessel "SHIYAN 1." In addition, the National Centers for Environmental Prediction reanalysis data used for the backward trajectory calculation and cluster analysis were obtained from the GDAS meteorological dataset (ARL, 2019) with a temporal resolution of 6 h and a spatial resolution of 1° × 1° (111 km × 111 km). The computer-based versions of HYSPLIT 4.2.0 and TrajStat 1.4.9 were used for the calculation of backward trajectories and for cluster analyses, respectively. The microplastic sampling stations and abundance distribution maps were drawn using Ocean Data View 5.2.0 and Microsoft Excel (2010). The deposition velocity model was calculated using R 3.6.1 (R Core Team, 2013). Spearman's correlation and principal component analysis were used to analyze the relationship between the abundance of atmospheric microplastics and meteorological parameters, generated using Origin version 2019b (OriginLab Corporation, Northampton, MA, USA). All data were tested for normality using the Shapiro-Wilk test to determine whether a parametric or non-parametric test was appropriate. Statistically significant differences were indicated by $p < 0.05$ in all tests.

3. Results and discussion

In our study, we implemented strict measures to prevent microplastic contamination during sampling and pre-treatment. No microplastics were found in the blank samples. Due to the extremely strong wind from October 7 to 8, 2019, the sampler was broken, and one sample was contaminated (Table S1). A total of 348 atmospheric samples were identified using Fourier transform infrared microspectroscopy (163 for active sampling and 185 for passive sampling). Of these, 295 samples were classified as plastics (135 for active sampling and 160 for passive sampling).

3.1. Microplastic distribution

Microplastics were detected in 12 atmospheric sampling transects over the northwestern South China Sea by active sampling, indirectly indicating higher atmospheric microplastic pollution in offshore areas. The abundance of microplastics in the atmosphere ranged from 0.013 to 0.063 n/m^3, with a median value of 0.032 n/m^3 and an average abundance of 0.035 ± 0.015 n/m^3 (Shapiro-Wilk test, $p = 0.822 > 0.05$) (Table S1). Overall, the abundance of microplastics increased as the distance from the coast decreased (Fig. 2).

The northern sampling area near the Pearl River Estuary is adjacent to the densely populated and industrially developed Pearl River Delta region creating the conditions for the production and use of plastics (Liu et al., 2019c). As shown in the backward trajectory graph, airflow can carry atmospheric pollutants over long distances across developed coastal cities along southeast China; thus, the abundance of microplastics was high in this area (Fig. S4). Owing to the relatively less intense industrial production in inland cities and the mountains acting as obstacles for the air to flow, the atmospheric microplastic abundance was slightly lower in the southern Pearl River Estuary. Similarly, the airflow traversing to eastern Hainan Island prevailed for longer over the ocean; therefore, the plastic pollutants carried from the cities were also lost during their transport, resulting in a lower abundance and fewer microplastic types. It is noteworthy that A11 (Fig. 2), which had high microplastic abundance, was clearly affected by human activities. The airflow that affected A11 passed through the Luzon Strait, which is a cargo transportation hub. Hence, the nearby ships release a large amount of plastic pollutants during their voyages. Meanwhile, Taiwan's plastics industry is essential for its rapid economic development (Xu, 1996). Also, the Philippines is one of the world's top three plastic waste manufacturers (Jambeck et al., 2015). Therefore, the aforementioned airflow may easily carry more plastic particles from Philippines located nearby and Taiwan.

The microplastic abundance recorded in this study was in the same order of magnitude as that recorded in Pearl River (0.042 n/m^3) (Wang et al., 2019) and higher than those recorded in the Eastern Indian Ocean (0.004 n/m^3) (Wang et al., 2019) and the Western Pacific (0.01 n/m^3) (Liu et al., 2019a) (Table S3). As both the Eastern Indian Ocean and the Western Pacific are situated far from human activity, some of the atmospheric microplastics are deposited or lost during long-distance transport. The atmospheric microplastic abundance recorded in this study was lower than those recorded in Zhongshan (0.077 n/m^3) (Liu et al., 2020) and Zhuhai (0.016 n/m^3) (Liu et al., 2020). Both Zhongshan and Zhuhai are located on the west coast of the Pearl River estuary, the abundance of atmospheric microplastics in these two cities is relatively high owing to the development of the plastics industry in the Pearl River Delta and the shipping industry. Overall, the atmospheric microplastic pollution over the northwestern South China Sea is lower than that in developed coastal cities and slightly higher than that in open oceans.

The results of the principal component analysis were consistent with Spearman's correlation results (Fig. 3, Table S4). The wind speed, atmospheric temperature, and pressure had a significant effect on the atmospheric microplastic abundance ($p < 0.05$), with a significantly negative correlation between temperature and abundance ($p = 0.049$) and a highly significant positive correlation between pressure, wind speed, and abundance ($p = 0.009$) (Fig. S5). The positive correlation of wind speed with microplastic abundance demonstrated that the long-distance transport of atmospheric microplastics required wind-driven conditions (Wang et al., 2019). Notably, we speculated that when the near-surface temperature decreased, the convective motion of the air was reduced and the atmospheric density increased. Thus, the air pressure increased, which led to a higher abundance of microplastics, as they were not easily dispersed. The explanation of the loading graph of the principal component analysis is presented in Text S9.

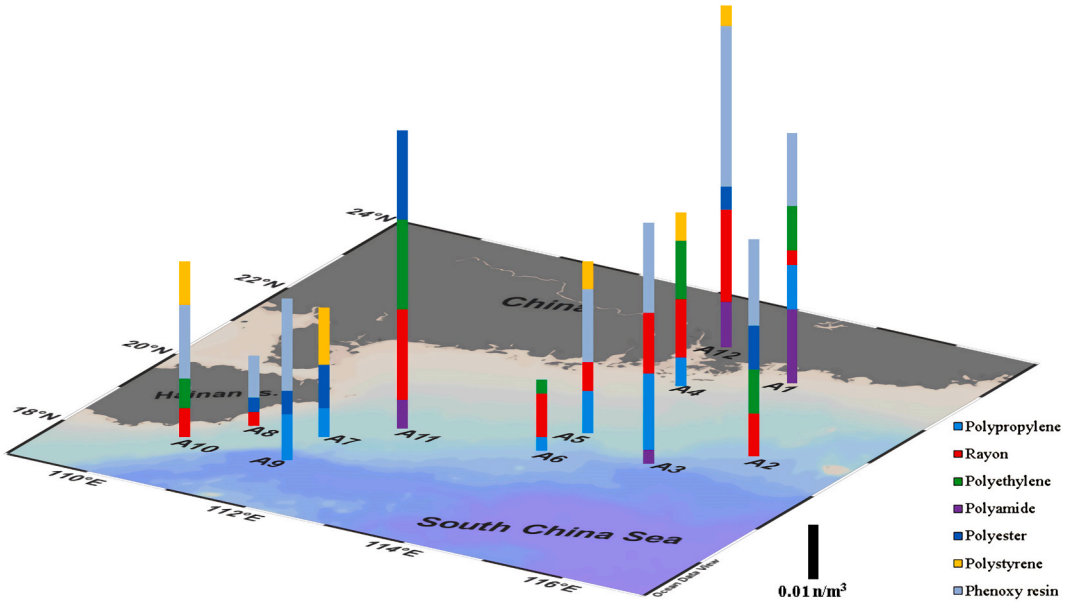

Fig. 2. Abundance and components of microplastics.

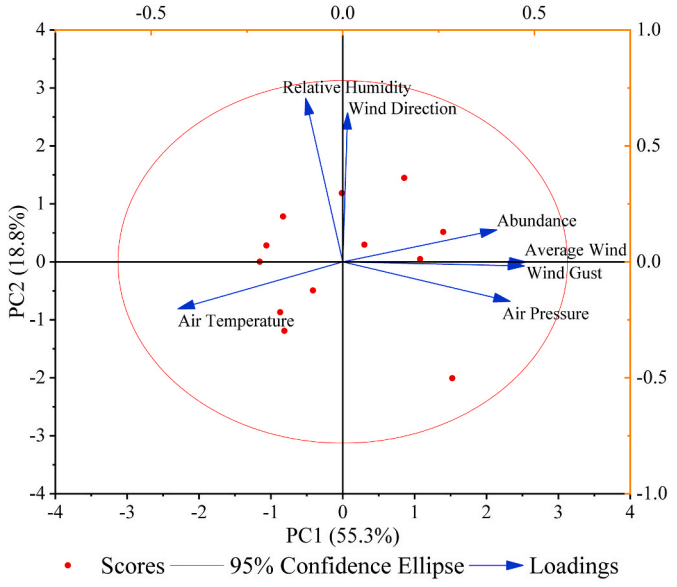

Fig. 3. Correlation between microplastic abundance and meteorological parameters recorded during the cruise.

3.2. Morphological features of microplastics

Atmospheric microplastics collected from active sampling were detected in six colors (Fig. 4a). Generally, the overall distribution of differently colored microplastics was even, with only slight differences (ranging from black 28% to red 9%). Differently shaped microplastics, such as granules, fibers, fragments, films, and foams, were detected in the atmosphere over the northwestern South China Sea (Fig. 4b). The shape of the microplastics detected was predominantly fibrous (65%), followed by fragments (20%) and granules (8%). Foams and films accounted for relatively small percentages of the total (4% and 3%, respectively). Two plastic microbeads were also observed. The fibrous microplastic is also the predominant shape reported in the literature (Chen et al., 2020), with very few studies reporting a higher proportion of fragments and granules (Abbasi et al., 2019; Klein and Fischer, 2019). This is likely because fibers may separate from certain products, such as clothing and ornaments. The quantity of fibrous microplastics in the environment may be related to the production of the corresponding products they originate in, and to a certain extent, can be used as a basis for determining the origin of the microplastics (Zhang et al., 2020).

The size of atmospheric microplastics ranged from 50 to 2210 μm (599 ± 513 μm; median = 405 μm). The particle size distribution graph showed that atmospheric microplastics were mainly in the size range of <200 μm (28%) (Fig. S6a). The microplastics in the size ranges of 200–500 μm (24%) and 500–1000 μm (26%) had similar distributions and accounted for half of the total when combined. Microplastics that were >2000 μm in size accounted for only 4% of the total.

The particle sizes of differently shaped microplastics were also analyzed statistically (Fig. 4d). The predominant size range of the granule, fragment, and foam shapes was <200 μm, which accounted for more than 70% of the total. Atmospheric microplastics were generally small, and all shapes were <1000 μm, except for fibers.

In this study, the predominant size range of atmospheric microplastics was 50–1000 μm, which is similar to the results reported in the literature. For instance, microplastics in Asaluyeh are <1000 μm (Abbasi et al., 2019), and those in the Pyrenees mountains (Allen et al., 2019), Western Pacific (Liu et al., 2019a), Paris (Dris et al., 2017), Dongguan (Cai et al., 2017), Shanghai (Liu et al., 2019c), and Yantai (Zhou et al., 2017) are < 500 μm in size. Our results indicate that the number of microplastics gradually increased and peaked as the particle size decreased (Fig. S6a). Owing to their smaller size and mass, atmospheric microplastics are easily suspended in the air and are more conducive to long-distance atmospheric transport (Helm, 2017).

3.3. Microplastic composition

Of samples collected by active sampling, seven polymer types were identified (polypropylene [PP], rayon [RY], polyethylene [PE], polyamide [PA], polyester [PES], polystyrene [PS], and phenoxy resin [PR]) (Fig. 4c).

PES accounted for the highest proportion (29%), followed by RY (19%). PP and PE had similar abundances and accounted for 15% and 13%, respectively, of the total. PS, PA, and PR were less abundant and together, accounted for <30% of the total. The two plastic beads were PE. In addition, natural fibers such as cellulose were detected.

The most common atmospheric microplastic type recorded in this study was PES, primarily comprising polyethylene terephthalate (PET),

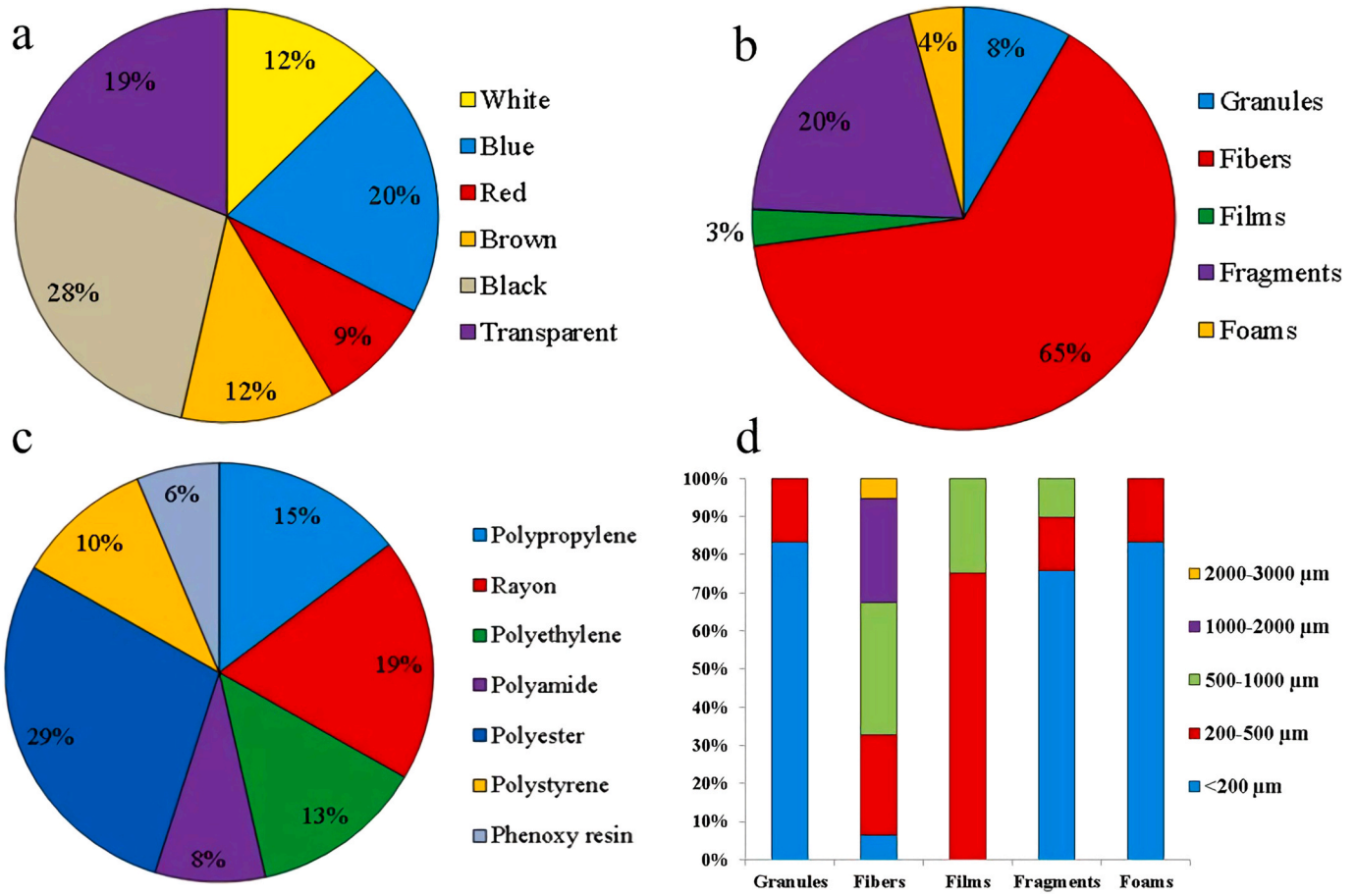

Fig. 4. a) Colors, b) shapes, c) composition of the components of microplastics, and d) the percentages of different size ranges for differently shaped microplastics. (For interpretation of the references to color in this figure legend, the reader is referred to the Web version of this article.)

polybutylene terephthalate (PBT), and polytrimethylene terephthalate (PTT). PES is widely used for packaging beverages, medicine, and chemical products for daily use (Song et al., 2014). Moreover, PES is an important synthetic fiber, which is mainly used in clothing and knitting. The increase in atmospheric PES may be related to the increase in global PES production. Additionally, current PES production accounts for more than half of the world's fiber production (Bywater and Yu, 2010); therefore, the PES recorded in this study may have originated from textile materials used for clothing and continued to decompose and degrade under the photo-oxidation effect. These ultrafine fibers float further through the resuspension process (Song et al., 2017). Similarly, RY and PA are often blended with other fibers to improve the wear resistance of the fabric, and thus, have a high probability of producing secondary microplastics (Liu et al., 2019c). PP and PE are currently the most widely produced plastics globally. Coastal cities in the southeast of China use these extensively as raw materials for the production of plastic products (Cai et al., 2017). PR is mainly used in the production of engineering plastics, such as paints and adhesives (Song et al., 2014). Such plastics are used in construction and can enter the atmosphere owing to mechanical breakage and physical tear.

3.4. Source analysis

The atmospheric backward trajectories of the 12 simulated reception points demonstrate the movement path of the airflow. Our results show that several sampling areas near the Pearl River Estuary were mainly influenced by the northeast winds passing through the southeast coast of China, with the airflow moving farther and faster, which corresponds to the higher surface wind speed and facilitated the transport of low-altitude pollutants over cities. The greater amounts of PP, PE, and PET detected in this region originated during industrial production, which is more prevalent in developed cities, thereby indicating that southeast coastal cities may be potential sources of atmospheric microplastics. The northerly airflow through other reception points in the southern Pearl River Estuary passes through China's inland cities and may also carry fewer air pollutants (Bretón et al., 2019). On eastern Hainan Island, the airflow through several simulated reception points was less influenced by the topography; thus, the recorded velocities had almost no differences, and the wind direction changed from northerly to easterly. In the vertical direction, the airflow was recorded at a fixed height with a small fluctuation frequency, which implies that the airflow affecting the sampling area had been moving slowly near the surface. The airflow passing through A11 through the Luzon Strait could be carrying a high quantity of air pollutants. Furthermore, the abundance of plastics and the high PA and RY percentages at this reception point suggest that the cities around the Luzon Strait constitute sources of atmospheric microplastics.

These results, combined with the cluster-mean back trajectories shown in Fig. 5, demonstrate that the airflow affecting the sampling area originated mainly in the northeast and may carry microplastics over cities in southeastern China into the South China Sea in the fall.

3.5. Contribution of the deposition of atmospheric microplastics in the oceans

A comparison of the microplastic sizes obtained by the two sampling methods showed no significant difference (Mann–Whitney U test, $p = 0.438 > 0.05$) (Fig. S6b). Because the passive sampling site was located

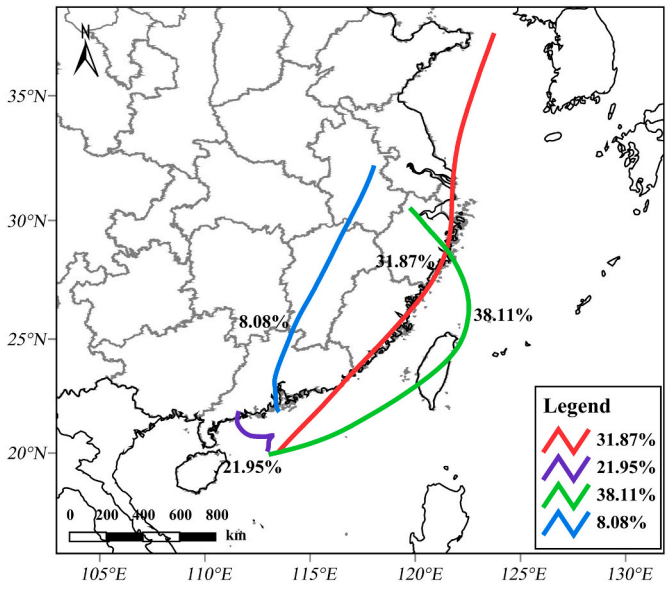

Fig. 5. Cluster-mean back trajectories recorded during sampling.

at the Pearl River Estuary, combined with the similarity in the composition and morphology of microplastics in the two regions (Table S3), the difference in atmospheric microplastics between the two sampling regions was small. This also validated the backward trajectory of the speculation on the direction of the main airflow affecting the active sampling region, which crossed northeastward inland China and carried microplastics over the city of Guangzhou to the South China Sea. Comparison of the dry deposition flux of three differently shaped microplastics with two sampling methods showed that the simulated results of the atmospheric dry deposition model used in this study were similar to the measured results, indicating the applicability of the model for flux calculations. Meanwhile, the amounts of microplastics collected during passive sampling were slightly larger than those obtained using active sampling, suggesting that microplastics over the ocean are less likely to be deposited when influenced by the wind. Moreover, the deposition flux in the study area was of the same order of magnitude as those in Paris (Dris et al., 2015, 2016, 2017), Hamburg (Klein and Fischer, 2019), Yantai (Zhou et al., 2017), the Pyrenees mountains (Allen et al., 2019), London (Wright et al., 2020), and protected lands in the western United States (Brahney et al., 2020). Additionally, we found that the deposition velocity of cylindrical microplastics (0.07 m/s) was less than those of flakes (0.08 m/s) and granules (0.15 m/s) (Text S6). This result was similar to that found in London, where the deposition velocities of fibers and non-fibers were 0.06 and 0.32 m/s, respectively (Wright et al., 2020), which is most likely because in our study, all cylindrical microplastics were fibers with a small relative mass and were more susceptible to suspension in the atmosphere for a longer time. This assumption was also verified by calculating the average mass of microplastics of different shapes.

We calculated the dry deposition of atmospheric microplastics in the northwestern South China Sea in the fall to be 1.4×10^3 t, which was higher than that in the protected areas of the western United States ($>2.5 \times 10^2$ t) (Brahney et al., 2020). Comparing the two studies, we considered that the difference was because the major particle size of microplastics (5–30 μm) detected in the United States was much smaller than that detected over the South China Sea in this study (50–1000 μm). This implies that smaller microplastic particles were more easily transported over long distances through the atmosphere. In addition, Mai et al. (2019) estimated the riverine input of microplastics from the Pearl River Delta to be 10.83 tons in the fall (the annual input was 66.1 tons) (0.3–5 mm). For microplastics <0.3 mm, owing to the lack of studies reported in the relevant region, we applied the findings on microplastic size in Changjiang estuary (Zhao et al., 2019) and estimated that < 0.3 mm microplastics accounted for 29.4% of total microplastics, and the mass of each < 0.3 mm microplastic particle was 0.000033 g. Then, we calculated that the total mass of <0.3 mm microplastics was approximately 0.166 tons. Therefore, the total riverine input of microplastics from the Pearl River Delta was approximately11 tons in the fall, which is significantly smaller than the amount from dry deposition of atmospheric microplastics. We conjectured that the total amount of the macroplastics (>5 mm) input from the river to the ocean was far more than that of microplastics. Mai et al. (2019) also calculated that the mass of macroplastics entering the South China Sea from the Pearl River Delta each year was 2.4×10^3–3.8×10^3 t, while Lebreton et al. (2017) used the model to estimate the input to be 1.09×10^4–2.31×10^4 t. Thus, in terms of the total amount of plastic, the difference between atmospheric and river transport is not significant, but the ability of the atmosphere to carry microplastics into the ocean is greater than that of rivers. Although macroplastics can eventually be broken into microplastics, the physical and chemical processes take a long time. Also, microplastics are more susceptible to the attachment of pathogenic microorganisms and ingested by organisms (Rochman et al., 2015; Zettler et al., 2013), it means that atmospheric microplastics are more likely to pose an ecological risk. Additionally, the contribution of atmospheric microplastic to the ocean cannot be ignored.

4. Conclusions

Overall, we studied the abundance, morphological characteristics, composition, and sources of atmospheric microplastics in the northwestern South China Sea. Furthermore, we also roughly estimated that the dry deposition of atmospheric microplastics into the ocean in the fall was 1.4×10^3 t. As the wet deposition of microplastics into the sea was not calculated in this study and the study area is only part of the South China Sea, the contribution of atmospheric microplastic deposition into South China Sea may be higher. Notably, both active and passive sampling methods had certain limitations, and we attempted to use a combination of the two methods to comprehensively assess atmospheric microplastic pollution, which should be followed by matching sampling at the same location and time to improve the accuracy of the sampling and the rigor of the data. Moreover, the accuracy of the Williams model for calculating the deposition velocity of atmospheric pollutants with longer particle sizes requires improvement. Therefore, long-term monitoring of atmospheric microplastics and the development of relevant evaluation standards are viable strategies for the reduction of amount of microplastics entering the ocean. In view of the complex transport process of microplastics in the atmosphere and the ocean, it is necessary to develop horizontal and depositional transport models according to the characteristics of microplastics.

CRediT authorship contribution statement

Yongcheng Ding: Conceptualization, Formal analysis, Investigation, Methodology, Data curation, Software, Visualization, Writing – original draft. **Xinqing Zou:** Funding acquisition, Conceptualization, Resources, Supervision, Project administration. **Chenglong Wang:** Investigation, Methodology. **Ziyue Feng:** Investigation. **Ying Wang:** Investigation. **Qinya Fan:** Investigation. **Hongyu Chen:** Investigation.

Declaration of competing interest

The authors declare that they have no known competing financial interests or personal relationships that could have appeared to influence the work reported in this paper.

Acknowledgements

This work was supported by National Natural Science Foundation of

China (NSFC) (41601560, 41849907) and the Postgraduate Research and Practice Innovation Program of Jiangsu Province (KYCX20_0029). We thank all the members of the scientific research vessel "SHIYAN 1" (NORC2019-07). We especially acknowledge support from Nian Tang for the identification of microplastics. We also acknowledge the helpful suggestions and comments from Yulong Yao and Weiwei Fang.

Appendix A. Supplementary data

Supplementary data to this article can be found online at https://doi.org/10.1016/j.atmosenv.2021.118389.

References

Abbasi, S., Keshavarzi, B., Moore, F., Turner, A., Kelly, F.J., Dominguez, A.O., Jaafarzadeh, N., 2019. Distribution and potential health impacts of microplastics and microrubbers in air and street dusts from Asaluyeh County, Iran. Environ. Pollut. 244, 153–164.

Air Resources Laboratory (ARL), 2019. GDAS meteorological dataset. June 2020. ftp://arlftp.arlhq.noaa.gov/pub/archives/gdas1.

Allen, S., Allen, D., Phoenix, V.R., Le Roux, G., Durántez Jiménez, P., Simonneau, A., Binet, S., Galop, D., 2019. Atmospheric transport and deposition of microplastics in a remote mountain catchment. Nat. Geosci. 12 (5), 339–344.

Balkanski, Y.J., Jacob, D.J., Bardner, G.M., 1993. Transport and residence times of tropospheric aerosols inferred from three-dimensional simulation of 210Pb. J. Geophys. Res. Atmospheres 98, 20573–20586.

Brahney, J., Hallerud, M., Heim, E., Hahnenberger, M., Sukumaran, S., 2020. Plastic rain in protected areas of the United States. Science 368 (6496), 1257–1260.

Brankov, E., Rao, S.T., Porter, P.S., 1998. A trajectory-clustering-correlation methodology for examining the long-range transport of air pollutants. Atmos. Environ. 32 (9), 1525–1534.

Bretón, R.M.C., Kahl, J., Bretón, J.G.C., Canul, J.A.S., 2019. The influence of Meteorology and atmospheric transport patterns on the sulfate levels in raiwater in orizaba valley, veracruz, Mexico. J. Environ. Protect. 10, 821–837, 06.

Bywater, N., Yu, Y., 2010. Global synthetic fibers market trends 2010-2020. Melliand China 6–8, 038(011).

Cai, L., Wang, J., Peng, J., Tan, Z., Zhan, Z., Tan, X., Chen, Q., 2017. Characteristic of microplastics in the atmospheric fallout from Dongguan city, China: preliminary research and first evidence. Environ. Sci. Pollut. Res. Int. 24 (32), 24928–24935.

Camarero, L., Bacardit, M., de Diego, A., Arana, G., 2017. Decadal trends in atmospheric deposition in a high elevation station: effects of climate and pollution on the long-range flux of metals and trace elements over SW Europe. Atmos. Environ. 167, 542–552.

Chen, G., Feng, Q., Wang, J., 2020. Mini-review of microplastics in the atmosphere and their risks to humans. Sci. Total Environ. 703, 135504.

Cózar, A., Echevarria, F., González-Gordillo, J.I., Irigoien, X., Úbeda, B., Hernández-León, S., Palma, A.T., Navarro, S., García-de-Lomas, J., Ruiz, A., Fernández-de-Puelles, M.L., Duarte, C.M., 2014. Plastic debris in the open ocean. Proc. Natl. Acad. Sci. U.S.A. 111, 10239–10244.

Crawford, C.B., Quinn, B., 2017. Microplastic separation techniques[M]//Microplastic pollutants. In: Crawford, C.B., Quinn, B. (Eds.), 10 - Microplastic Identification Techniques. Microplastic Pollutants. Elsevier, pp. 219–267.

Dris, R., Gasperi, J., Mirande, C., Mandin, C., Guerrouache, M., Langlois, V., Tassin, B., 2017. A first overview of textile fibers, including microplastics, in indoor and outdoor environments. Environ. Pollut. 221, 453–458.

Dris, R., Gasperi, J., Rocher, V., Saad, M., Renault, N., Tassin, B., 2015. Microplastic contamination in an urban area: a case study in greater paris. Environ. Chem. 12 (5), 592.

Dris, R., Gasperi, J., Saad, M., Mirande, C., Tassin, B., 2016. Synthetic fibers in atmospheric fallout: a source of microplastics in the environment? Mar. Pollut. Bull. 104 (1–2), 290–293.

Evangeliou, N., Grythe, H., Klimont, Z., Heyes, C., Eckhardt, S., Lopez-Aparicio, S., Stohl, A., 2020. Atmospheric transport is a major pathway of microplastics to remote regions. Nat. Commun. 11 (1), 3381.

GESAMP, 2016. Sources, Fate and Effects of Microplastics in the Marine Environment: Part 2 of a Global Assessment. IMO/FAO/UNESCO-IOC/UNIDO/WMO/IAEA/UN/UNEP/UNDP Joint Group of Experts on the Scientifc Aspects of Marine Environmental Protection.

Geyer, R., Jambeck, J.R., Law, K.L., 2017. Production, use, and fate of all plastics ever made. Sci. Adv. 3 (7), e1700782.

Guo, X., Cai, X., Xin, G., 2005. Analytical solution of the length of the stable near–surface layer Monin-Obukhov. Acta Sci. Nauralium Univ. Pekin. 41 (2) (in Chinese).

He, Y.K., 2016. Correlation analysis of marine atmospheric process characteristics in the northwest of the South China Sea. Doctor Thesis. The Graduate School of The Chinese Academy of Sciences, Guangzhou. China.

Helm, P.A., 2017. Improving microplastics source apportionment: a role for microplastic morphology and taxonomy? Anal. Methods 9, 1328–1331.

Hidalgo-Ruz, V., Gutow, L., Thompson, R.C., Thiel, M., 2012. Microplastics in the marine environment: a review of the methods used for identification and quantification. Environ. Sci. Technol. 46, 3060–3075.

Huang, Y., Qing, X., Wang, W., Han, G., Wang, J., 2020. Mini-review on current studies of airborne microplastics: analytical methods, occurrence, sources, fate and potential risk to human beings. Trac. Trends Anal. Chem. 125.

Inter-Agency Committee, 1957. Some fundamentals of particle size analysis: a study of methods used in measurement and analysis of sediment loads in streams. In: Rep. No. 12, Subcommittee on Sedimentation, Interagency Committee on Water Re-sources. St. Anthony Falls Hydraulic Laboratory, Minneapolis.

Jambeck, J.R., Geyer, R., Wilcox, C., Siegler, T.R., Perryman, M., Andrady, A., Narayan, R., Law, K.L., 2015. Marine pollution. Plastic waste inputs from land into the ocean. Science 347 (6223), 768–771.

Jiang, H., Yin, Y., Wang, X., Gao, R., Yuan, L., Chen, H., Shan, Yun, 2016. The measurement and parameterization of ice nucleating particles in different backgrounds of China. Atmos. Res. 181, 72–80.

Jiang, P., Zhao, S., Zhu, L., Li, D., 2018. Microplastic-associated bacterial assemblages in the intertidal zone of the yangtze estuary. Sci. Total Environ. 624, 48–54.

Käppler, A., Fischer, D., Oberbeckmann, S., Schernewski, G., Labrenz, M., Eichhorn, K.J., Voit, B., 2016. Analysis of environmental microplastics by vibrational microspectroscopy: ftir, Raman or both? Anal. Bioanal. Chem. 408 (29), 1–15.

Kiessling, T., Gutow, L., Thiel, M., 2015. Marine litter as habitat and dispersal vector. In: Bergmann, M., Gutow, L., Klages, M. (Eds.), Marine Anthropogenic Litter. Springer, Berlin, pp. 141–181.

Klein, M., Fischer, E.K., 2019. Microplastic abundance in atmospheric deposition within the Metropolitan area of Hamburg, Germany. Sci. Total Environ. 685, 96–103.

Kukulka, T., Proskurowski, G., Morét-Ferguson, S., Meyer, D.W., Law, K.L., 2012. The effect of wind mixing on the vertical distribution of buoyant plastic debris. Geophys. Res. Lett. 39 (7).

Lebreton, L.C.M., van der Zwet, J., Damsteeg, J.W., Slat, B., Andrady, A., Reisser, J., 2017. River plastic emissions to the world's oceans. Nat. Commun. 8, 15611.

Lenz, R., Enders, K., Stedmon, C.A., Mackenzie, D.M.A., Nielsen, T.G., 2015. A critical assessment of visual identification of marine microplastic using Raman spectroscopy for analysis improvement. Mar. Pollut. Bull. 100 (1), 82–91.

Liu, K., Wang, X., Fang, T., Xu, P., Zhu, L., Li, D., 2019c. Source and potential risk assessment of suspended atmospheric microplastics in Shanghai. Sci. Total Environ. 675, 462–471.

Liu, K., Wang, X., Wei, N., Song, Z., Li, D., 2019b. Accurate quantification and transport estimation of suspended atmospheric microplastics in megacities: implications for human health. Environ. Int. 132, 105127.

Liu, K., Wu, T., Wang, X., Song, Z., Zong, C., Wei, N., Li, D., 2019a. Consistent transport of terrestrial microplastics to the ocean through atmosphere. Environ. Sci. Technol. 53 (18), 10612–10619.

Liu, K., Wang, X., Song, Z., Wei, N., Ye, H., Cong, X., Zhao, L., Li, Y., Qu, L., Zhu, L., Zhang, F., Zong, C., Jiang, C., Li, D., 2020. Global inventory of atmospheric fibrous microplastics input into the ocean: an implication from the indoor origin. J. Hazard Mater. 400, 123223.

Lo, K.F., Zhang, L., Sievering, H., 1999. The effect of humidity and state of water surfaces on deposition of aerosol particles onto a water surface. Atmos. Environ. 33 (28), 4727–4737.

Ma, Y., Li, M., Ju, C., Yu, X., Li, S., Xin, Y., 2015. Simulation of airflow trajectories in the Taklamakan desert. J. Arid Land Resour. Environ. 29 (7) (in Chinese).

Mai, L., You, S.N., He, H., Bao, L.J., Liu, L.Y., Zeng, E.Y., 2019. Riverine microplastic pollution in the Pearl River Delta, China: are modeled estimates accurate? Environ. Sci. Technol. 53 (20), 11810–11817.

Mecozzi, M., Pietroletti, M., Monakhova, Y.B., 2016. FTIR spectroscopy supported by statistical techniques for the structural characterization of plastic debris in the marine environment: application to monitoring studies. Mar. Pollut. Bull. 106 (1–2), 155–161.

Moore, C.J., 2008. Synthetic polymers in the marine environment: a rapidly increasing, long-term threat. Environ. Res. 108 (2), 0–139.

Peng, J., Wang, J., Cai, L., 2017. Current understanding of microplastics in the environment: occurrence, fate, risks, and what we should do. Integrated Environ. Assess. Manag. 13 (3), 476–482.

Pidwirny, M., 2011. Köppen climate classifcation system. Accessed June 2020. https://www.slideshare.net/KellaRandolph/koppen-classifcation-system.

Plastic Europe K, 2019. Plastic Europe unveils updated plastics data and voluntary commitment progress. https://www.plasticseurope.org/en/newsroom. October 2019.

Rochman, C.M., Tahir, A., Williams, S.L., Baxa, D.V., Lam, R., Miller, J.T., The, F.C., Werorilangi, S., The, S.J., 2015. Anthropogenic debris in seafood: plastic debris and fibers from textiles in fish and bivalves sold for human consumption. Sci. Rep. 5, 14340.

Song, Y.K., Hong, S.H., Jang, M., Han, G.M., Jung, S.W., Shim, W.J., 2017. Combined effects of UV exposure duration and mechanical abrasion on microplastic fragmentation by polymer type. Environ. Sci. Technol. 51 (8), 4368–4376.

Song, Y.K., Hong, S.H., Jang, M., Kang, J.H., Kwon, O.Y., Han, G.M., Shim, W.J., 2014. Large accumulation of micro-sized synthetic polymer particles in the sea surface microlayer. Environ. Sci. Technol. 48 (16), 9014–9021.

State Oceanic Administration (SOA), 2015. Technical protocols for the assessment of atmospheric pollutant deposition fluxes into the sea. October 2015. http://gc.mnr.gov.cn/201807/t20180710_2079009.html.

Sun, Zh, Meng, L., Gao, H., Wang, J., 2018. Use of satellite data to invert aerosol concentrations and dry deposition fluxes off the coast of China. Period. Ocean Univ. China 48 (3), 030–040 (in Chinese).

Wang, X., Li, C., Liu, K., Zhu, L., Song, Z., Li, D., 2019. Atmospheric microplastic over the south China Sea and East Indian ocean: abundance, distribution and source. J. Hazard Mater. 121846.

Wang, Z.J., 2006. Study on dry deposition model of atmospheric aerosol and dry deposition fluxes of elements loaded on aerosol to the sea near Qingdao area. Master Thesis. Ocean University of China, Qingdao. China.
Williams, R.M., 1982. A model for the dry deposition of particles to natural water surfaces. Atmos. Environ. 16, 1933–1938.
World Economic Forum, 2016. The new plastics economy: rethinking the future of plastics, 2016. http://www3.weforum.org/docs/WEF_The_New_Plastics_Economy.pdf.
Wright, S.L., Ulke, J., Font, A., Chan, K.L.A., Kelly, F.J., 2020. Atmospheric microplastic deposition in an urban environment and an evaluation of transport. Environ. Int. 136, 105411.
Xu, Zh, 1996. Current situation of taiwan's plastics industry, 01 Chem. Ind. Times 34–35 (in Chinese).
Zettler, E.R., Mincer, T.J., Amaral-Zettler, L.A., 2013. Life in the "plastisphere": microbial communities on plastic marine debris. Environ. Sci. Technol. 47 (13), 7137–7146.
Zhan, J., Chen, L., Zhang, Yuan, Yang, X., Li, W., Lin, Q., Du, J., Lin, H., 2010. Study of dry deposition flux of aerosols at the sea surface in the Taiwan Strait. J. Oceanogr. Taiwan Strait 29 (2) (in Chinese).
Zhang, Ch, Zhou, W., 1995. Atmospheric Aerosols Course. Meteorological Press, Beijing. China, pp. 13–32.
Zhang, Y., Gao, T., Kang, S., Sillanpaa, M., 2019. Importance of atmospheric transport for microplastics deposited in remote areas. Environ. Pollut. 254 (Pt A), 112953.
Zhang, Y., Kang, S., Allen, S., Allen, D., Gao, T., Sillanpää, M., 2020. Atmospheric microplastics: a review on current status and perspectives. Earth Sci. Rev. 203.
Zhao, S., Wang, T., Zhu, L., Xu, P., Wang, X., Gao, L., Li, D., 2019. Analysis of suspended microplastics in the Changjiang Estuary: implications for riverine plastic load to the ocean. Water Res. 161, 560–569.
Zhao, S., Zhu, L., Wang, T., Li, D., 2014. Suspended microplastics in the surface water of the Yangtze Estuary System, China: first observations on occurrence, distribution. Mar. Pollut. Bull. 86, 562–568.
Zhou, Q., Tian, C., Luo, Y., 2017. Various forms and deposition fluxes of microplastics identified in the coastal urban atmosphere. Chin. Sci. Bull. 62 (33), 3902–3910 (in Chinese).
Zhu, S., Zhou, M., Qiao, L., L, L., L, S., Y, R., W, H., T, S., C, C., 2016. Impact of the air mass trajectories on PM2.5 concentrations and distribution in the Yangtze River Delta in December 2015. Acta Sci. Circumstantiae 36 (12), 4285–4294.